HIGH EFFICIENCY AND LOW COST POWER AMPLIFIERS AND TRANSDUCERS FOR ACTIVE MAGNETIC BEARINGS

Flavio Cerruti*, Cristiana Delprete, Giancarlo Genta
Dipartimento di Meccanica, Politecnico di Torino, Torino, Italia
Stefano Carabelli
Dipartimento di Automatica e Informatica, Politecnico di Torino, Torino, Italia

ABSTRACT
The implementation of commercially oriented rotating devices based on active magnetic bearings may be promoted by the availability of low cost and high efficiency actuators and transducers. The aim of the present paper is to show some results on the subject. A class G amplifier and a co-located inductive position sensor have been theoretically studied and experimentally tested on the test rig built at the Dipartimento di Meccanica of Politecnico di Torino. The simultaneous use of the realised co-located transducer and of a switching power amplifier may cause strong interference problems; this issue is currently being investigated.

LINEAR POWER AMPLIFIER
Originally a linear transconductance amplifier has been build and tested. In order to improve the overall efficiency of the amplifier loaded by the high inductance and low resistance typical of the electrical load of the magnetic bearing coil, a class G amplifier has been developed. A couple of power Darlington pairs is connected on the same load but supplied with different voltages: the higher to deal with the inductive transient and the lower with the resistive steady state. The choice of the ratio of the two supply voltages is carried out assuming a varying component of the driving current synchronous with the spin speed.

Motivation
The use of linear transconductance amplifiers to drive the coils of magnetic bearings may be still the lowest cost solution for light and high spin speed rotating machines while switched power amplifiers either analogically or digitally driven is surely to be chosen for heavier applications [1]. Moreover linear amplifiers are intrinsically less noisy than switched ones and this fact represents an advantage in the design and the operation of co-located inductive sensors like that described in the second part of the paper.
Given the standard amplifier connections for each axis of a magnetic bearing shown in figure 1, a so-called class A actuator arrangement [2] is adopted: both amplifiers are always activated simultaneously. Its main advantage is the physical linearization of the current-force action, its major drawback the need to use high bias currents (half of the maximum current) in order to eliminate the anisotropy typical of a class B actuator [3] (with only one amplifier activated at a time).

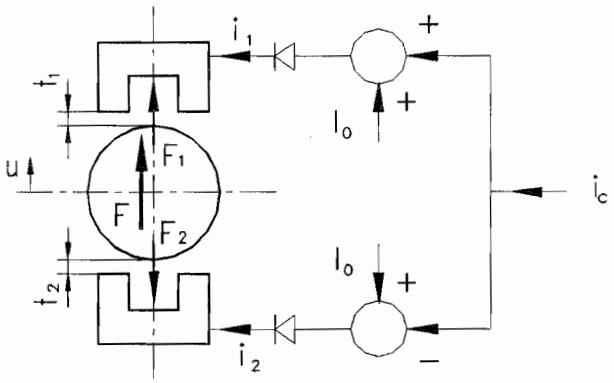

FIGURE 1: Magnetic bearing scheme. The diode symbol means that the current amplifier must go off for negative currents.

* At present with GOMA Elettronica s.r.l., Torino, Italia.

The working conditions here assumed are characterised by the high stiffness required to the magnetic bearings (typical for spindles for machine tools): the synchronous unbalance forces must be counteracted by the magnetic bearing thrust produced by a synchronous sinusoidal control current in the electromagnetic coils

$$i_c(t) = I_c \sin(\omega t) \tag{1}$$

where ω is the angular speed and I_C is proportional to the unbalance force

$$F_{unbal} = m\varepsilon\omega^2 \tag{2}$$

with m the rotor mass and ε the eccentricity.
Using the usual linearized expression for the actuating control force

$$F_c(t) = k_i i_c(t) + k_u u(t) \tag{3}$$

the following expression is obtained

$$I_c = \frac{|F_{unbal}|}{4\frac{K}{t_0^2} I_0} = \frac{m t_0^2}{4KI_0}\varepsilon\omega^2 \tag{4}$$

with t_0 the nominal air gap and K the electromagnetic constant that takes into account all the constructive bearing parameters.
The overall current is then

$$i(t) = I_0 + i_c(t) \tag{5}$$

where I_0 is the bias current, usually taken as half of i_{max}.

Actuator efficiency

In order to evaluate and compare different amplifier configurations, i.e. class A, class G or even class D, an efficiency index is defined according to the particular characteristic of the impedance load constituted by the electromagnetic coils: high inductance and low resistance.
The low resistance (usually below 1 Ω) requires a sort of "reactive amplifier" where the maximum current to be supplied is determined by the maximum load force to be coped with and the maximum voltage is determined by the force slew rate, i.e. its maximum derivative.
The amplifier maximum power is then defined as

$$P_{a\,max} = V_{max} I_{max} \tag{6}$$

The amplifier efficiency for use with active magnetic bearing actuators may be conveniently defined as follows

$$\eta_{AMB} = \frac{P_{a\,max}}{P_{a\,max} + P_d} \tag{7}$$

where P_d is the average loss power.
Acting on an almost pure inductive load the average supplied power $\overline{P_{al}}$ is almost completely dissipated on the power transistors, namely it coincides with the usually defined loss power $P_d \cong \overline{P_{al}}$.

Class G amplifier

A power amplifier is rated as class G when it has at least two different voltage supplies to work with. It is understood that, in the case of the coil load, the lower should address mainly the resistive and low reactive demand while the higher comes into action otherwise. The ratio between the two supply voltages

$$\alpha = \frac{V_{cc\,low}}{V_{cc\,high}} \tag{8}$$

should be chosen accordingly to the efficiency η_{AMB} previously defined. It should be noticed that a class G amplifier becomes a class A amplifier when α goes to one. The instantaneous supplied power is defined as

$$P_{al}(t) = \begin{cases} V_{cc}\, i(t) & \text{for } v(t) > \alpha V_{cc} \\ \alpha V_{cc}\, i(t) & \text{for } v(t) \le \alpha V_{cc} \end{cases} \tag{9}$$

where v is the voltage across the load impedance (neglecting the drop-out voltage of the amplifiers).
The voltage across the load $Z = R + j\omega L$ is

$$v(t) = |Z| I_c \sin(\omega t + \angle Z) + RI_0 \tag{10}$$

As already noted, it is assumed that $\omega L >> R$ and thus

$$|Z| \cong \omega L \qquad \angle Z \cong \pi/2 \tag{11}$$

The average supplied power is thus the following (see figure 2)

$$\overline{P_{al}} = \frac{V_{cc} I_0}{T}\left[2\tau(1-\alpha) + \alpha T\right] \tag{12}$$

where $T = 2\pi/\omega$ and τ represents the part of the period T when the higher supply voltage comes into play.
Using conditions (11) and equation (12) for $t = \tau$, it is possible to obtain the following expression for τ

$$\tau = \frac{T}{2\pi}\text{acos}\left(\frac{\alpha V_{cc}}{\omega L I_c}\right) \tag{13}$$

and the switching condition between the two supplies

$$I_{c\,\text{switch}} = \frac{\alpha V_{cc} - RI_0}{|Z|} \cong \frac{\alpha V_{cc} - RI_0}{\omega L} \cong \frac{\alpha V_{cc}}{\omega L} \quad (14)$$

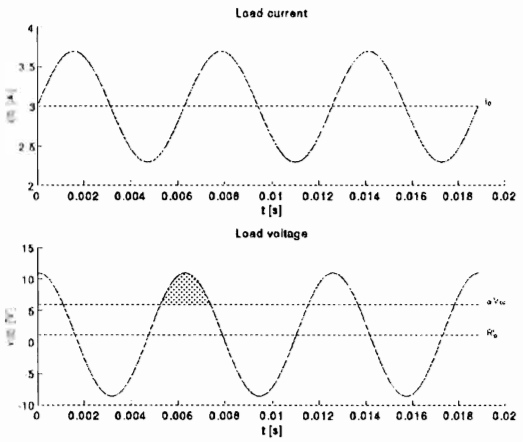

FIGURE 2: Load current and voltage. The marked area corresponds to the high supply voltage activity, lasting for time τ out of T. ($_{cc}$ = 40 V, α = 0.15).

Figure 3 shows the average supplied power $\overline{P_{al}}$ as a function of I_c for various α.

The horizontal asymptotes on the left hand side are easily computed for $\tau = 0$ and correspond to the situation where the voltage on the load never goes higher than the lower supply voltage αV_{cc}

$$\overline{P}_{al\,\text{left}} = \alpha V_{cc} I_0 \quad . \quad (15)$$

The horizontal asymptotes on the right hand side are obtained for the current going to infinity

$$\overline{P}_{al\,\text{right}} = \frac{\alpha + 1}{2} V_{cc} I_0 \quad . \quad (16)$$

For what the parameter α is concerned a critical lower condition is reached when the lower supply voltage is less than the voltage across the resistive part of the load

$$\alpha_{\text{inf}} V_{cc} = RI_0 \quad (17)$$

that has an obvious physical meaning: the lower supply never comes into play. On the other extreme an interesting upper value α_{sup} is obtained at the intersection of the α_{inf} curve and a generic left asymptote in $I_{c\,\text{switch}}$. It represents a critical upper value above which the average loss power is always increasing with α for any value of the unbalance current.

Figure 4 shows the efficiency η_{AMB} as a function of the control current I_c for various α. Figure 5 shows the average supplied power for $\alpha \in (\alpha_{\text{inf}}, \alpha_{\text{sup}})$. It should be clear that the choice of α depends on the maximum

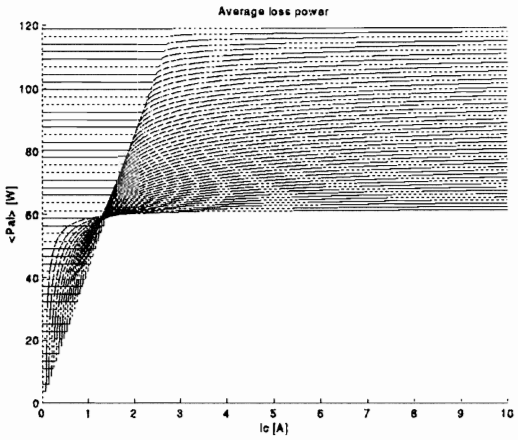

FIGURE 3: Average supplied power. Curves grow up for increasing α.

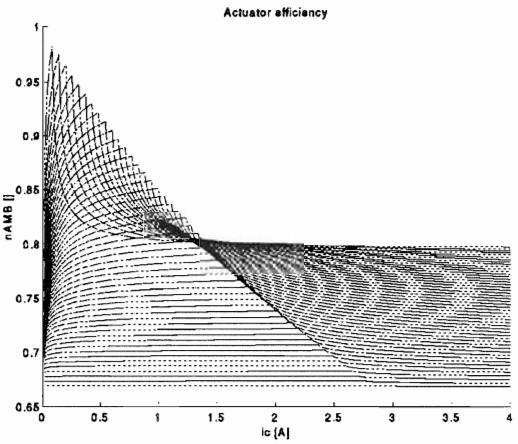

FIGURE 4: Active magnetic bearing efficiency. Curves grow down for increasing α.

allowable unbalance: the shaded area represents the trade off between two different choices of α. Figure 6 shows the curves of the efficiency η_{AMB} as a function of α for different control currents I_c.

CO-LOCATED POSITION SENSOR

The original position transducer used was a commercially available eddy current proximity sensor. Apart from its cost, it cannot be co-located with the relevant actuator. A co-located inductive sensor has been designed and built using the same polar expansions of the radial actuators. An impedance bridge with a modulator-demodulator configuration is used to extract the signal related to the position information.

Principles

The basic layout of a radial position sensor composed by two couples of faced coils is proposed (fig. 7).

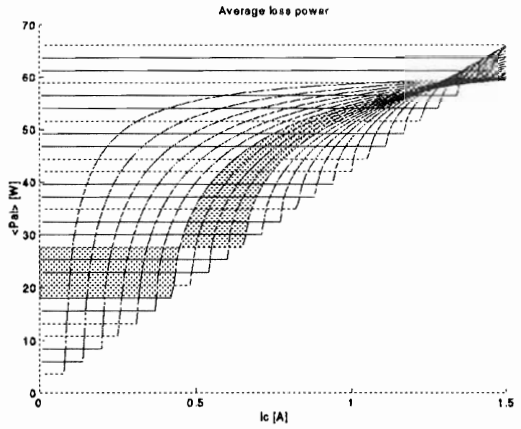

FIGURE 5: Average supplied power for $\alpha \in (\alpha_{inf}, \alpha_{sup})$.

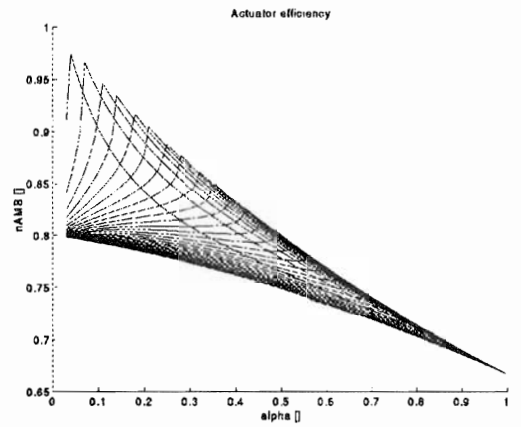

FIGURE 6: Active magnetic bearing efficiency. Curves grow down for increasing I_c.

At the nominal gap case the air gaps are all equal

$$t_1 = t_2 = t_3 = t_4 = t_0 \tag{18}$$

while a displacement u along a co-ordinate axis causes

$$\begin{aligned} t_1 &= t_0 + u \\ t_3 &= t_0 - u \\ t_2 &= t_4 = t_0 \quad \text{for any } u \end{aligned} \tag{19}$$

The magnetic flux associate with a single coil is sketched in figure 8.
The inductance of the single coil is related to the total reluctance of its concatenated magnetic flux

$$L = \frac{N}{\Re_{tot}} \tag{20}$$

with N the number of turns. Under the assumption of no magnetic losses in the iron body, the total reluctance of the magnetic circuit is due to the air gaps only (fig. 9)

$$\Re_{tot} = \Re_1 + \Re_2 \| \Re_3 \| \Re_4 \tag{21}$$

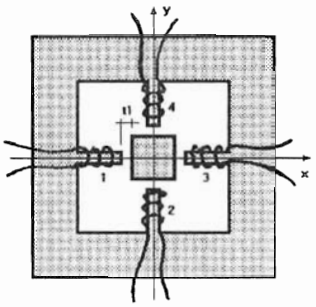

FIGURE 7: Radial position inductive sensor

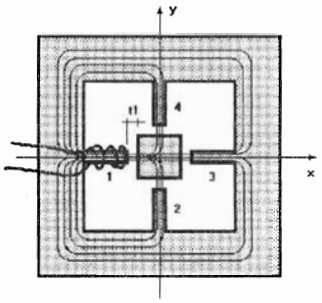

FIGURE 8: Magnetic flux for a single coil

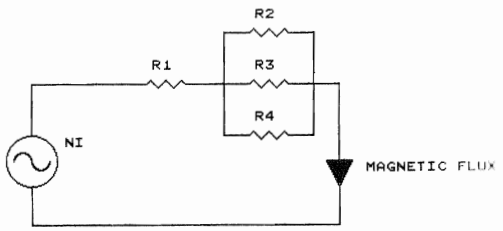

FIGURE 9: Electric equivalent of the magnetic circuit corresponding to a single coil.

From the definition of the magnetic reluctance (in air)

$$\Re = \frac{1}{\mu_0}\frac{t_0}{S} \tag{22}$$

with μ_0 the magnetic permeability for vacuum or air and S the gap section, and introducing the definitions

$$\Re_t = \frac{1}{\mu_0}\frac{t_0}{S} \qquad \Re_u = \frac{1}{\mu_0}\frac{u}{S} \tag{23}$$

it is possible to calculate the total reluctance and then the inductance for coil 1

$$\Re_{tot} = \frac{2\Re_u^2 - 4\Re_t}{2\Re_u - 3\Re_t} = \frac{1}{\mu_0 S}\frac{2u^2 - 4t_0^2}{2u - 3t_0} \qquad (24)$$

$$L_1 = N\mu_0 S \frac{2u - 3t_0}{2u^2 - 4t_0^2} \quad . \qquad (25)$$

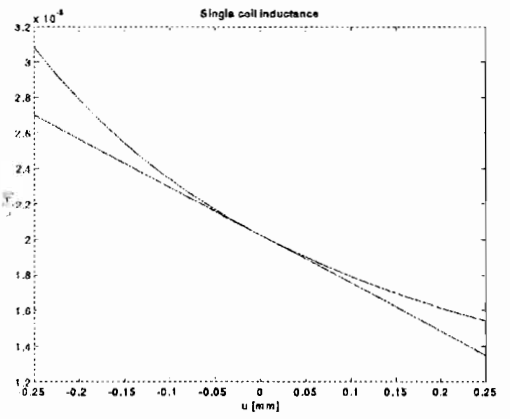

FIGURE 10: Coil inductance as a function of the gap displacement ($S = 1$ cm^2, $t_0 = 0.5$ mm, $N = 100$).

Figure 10 shows that the expression for the inductance is fairly linear for reasonable values of the displacement.
The linearized expression of the inductance around the equilibrium position ($u = 0$) is then

$$L = N\mu_0 S\left(\frac{3}{4t_0} - \frac{1}{2t_0^2}u\right) \quad . \qquad (26)$$

Due to the system symmetry, it is straitforward to obtain the expression of the inductance of the other three coils.
Note that in practice four coils are always used, two for each axis: even if the inductive sensor can work with only two coils, one for each axis, it is very important to use the two coils placed on the same axis in a differential configuration. In fact the differential configuration is essential in suppressing the intermodulation between axes due to mutual inductance (i.e. a variation of inductance of coil 2 and 4 due to a movement of the central piece of material along the *x*-axis) and in reducing the sensitivity to external noise.

Signal conditioning

Once demonstrated the dependence of the inductance to the displacement, it is necessary to obtain a voltage signal carrying the position information. This task is accomplished supplying a carrier signal to the bridge at a frequency where the inductance is dominant with respect to the resistance (usually very small) of the sensor coils, that is $2\pi fL >> R$ (fig. 11).

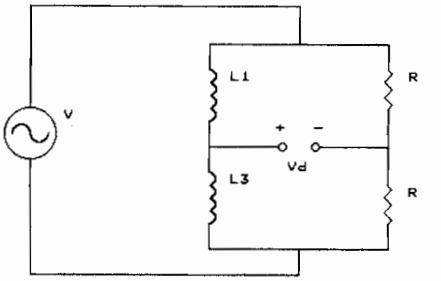

FIGURE 11: Sensor bridge.

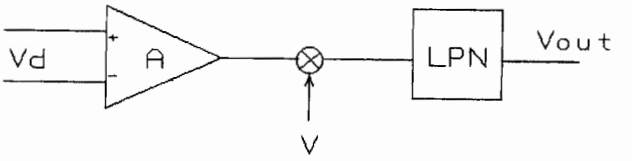

FIGURE 12: Principle of coerent demodulation.

Using the expression (26) for the inductances L_1 and L_3 and the new defined quantities

$$L_t = \frac{3}{4}\frac{N\mu_0 S}{t_0} \qquad L_u = \frac{N\mu_0 S}{2t_0^2}u \qquad (27)$$

it is possible to write

$$L_1 = L_t - L_u \qquad L_3 = L_t + L_u \qquad (28)$$

and then the voltage signal as a function of the displacement

$$V_u = \frac{L_u}{2L_0}V = \frac{V}{3t_0}u \qquad (29)$$

where V is the carrier sinusoidal signal for a standard coerent demodulation circuit whose scheme of principle is depicted in figure 12. The low-pass notch filter LPN must be centred on a frequency twice that of the sinusoidal generator.

Co-location

The advantage of the inductive sensor above described is that it is possible to build a co-located position transducer simply by adding four windings to an active magnetic bearing using the same magnetic core of the actuator as illustrated by figure 13. The figure clearly shows the flux of the magnetic field relative to the

actuator which uses the same core of coil 1: it is evident that the flux is not concatenated with the coil of the sensor.

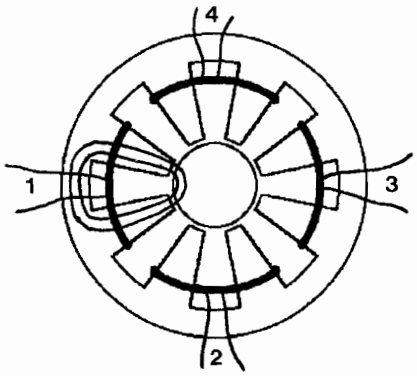

FIGURE 13: Co-located inductive sensor layout with concatenated magnetic fluxes.

Limitations

The inductive co-located position transducer bandwidth is limited by the parasitic capacitance always present in parallel with the coil inductance. Its main effect is to introduce a phase shift that corrupts the measure.

Another assumption for the transducer to work properly is the linearity of the B-H curve of the magnetic material. In order to accomplish this assumption much care must be used in the choice of the active magnetic actuator bias current. The interference with actuator activity may be more than a problem when co-located sensors are used in conjunction with power switching amplifiers: the relative frequency placement of the carrier generators should be carefully addressed (fig. 14).

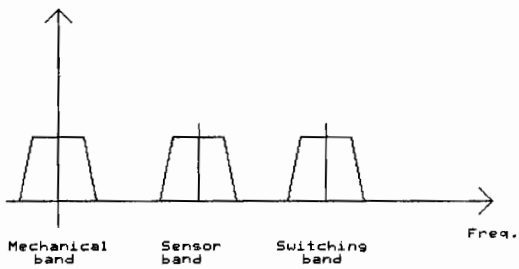

FIGURE 14: Relative placement of "mechanical", sensor and actuator bands.

Experimental results

The inductive position transducer has been calibrated on the test rig built in the Mechatronics Lab of Politecnico di Torino [4]. A first test was carried out with the rotor statically positioned at the nominal equilibrium position (fig. 15). The transducer resolution is around the micrometer for a range that comprises the whole nominal air gap. A second test was carried out in the same condition except for a bias current in the actuators. The results are almost identical with those of the first test for small displacement around the nominal position and differ from the preceding ones only by a 5% at the extreme of the position range.

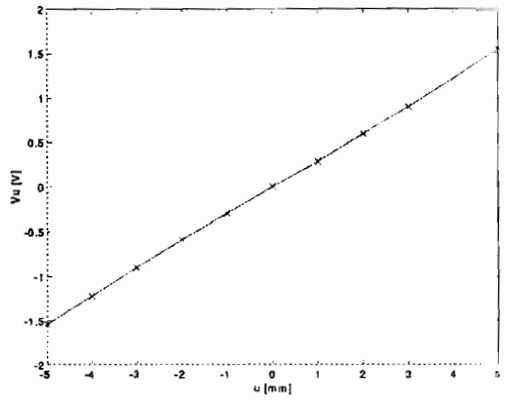

FIGURE 15: Experimental results of the co-located inductive position sensor.

CONCLUSIONS

The results reported in the present paper show that a deeper understanding of the actuating and transducing subsystems of an active magnetic bearing may lead to interesting results in terms of hardware costs.

In the authors' opinion this kind of approach may well contribute to the wide spread of magnetic bearing technology to many other fields today still untouched.

The availability of a test rig designed and built looking forward to practical commercial applications has proved crucial to validate several theoretical insights on the subjects.

REFERENCES

[1] Keith F.J., Maslen E.H., Hunphris R.R. and Williams R.D., Switching Amplifier Design for Magnetic Bearings, Proc. of 2nd Int. Symp. on Magnetic Bearings, Japan, 1990.

[2] Schröder U., Power Amplifier for Magnetic Bearings, A Short Course on Magnetic Bearings, France, 1993.

[3] Delprete C., Genta G. and Carabelli S., Control Strategies for Decentralised Control of Active Magnetic Bearings, Proc. of 4th Int. Symp. on Magnetic Bearings, Switzerland, 1994.

[4] Delprete C., Genta G. and Carabelli S., Design, Construction and Testing of a Five-Active Axes Magnetic Bearing System, Proc. of 2nd Int. Symp. on Magnetic Suspension Technology, Washington, 1993.